British Journal of Pharmacology (2008) 154, 1104–1115
 0007–1188/08 $30.00
www.brjpharmacol.org

RESEARCH PAPER

Characterization of a CNS penetrant, selective M_1 muscarinic receptor agonist, 77-LH-28-1

CJ Langmead[1], NE Austin[1], CL Branch[1], JT Brown[2], KA Buchanan[3], CH Davies[1], IT Forbes[1], VAH Fry[1], JJ Hagan[1], HJ Herdon[1], GA Jones[1], R Jeggo[4], JNC Kew[1], A Mazzali[5], R Melarange[1], N Patel[1], J Pardoe[1], AD Randall[2], C Roberts[1], A Roopun[6], KR Starr[1], A Teriakidis[2], MD Wood[1], M Whittington[6], Z Wu[7] and J Watson[1]

[1]*Psychiatry Centre of Excellence for Drug Discovery, GlaxoSmithKline, Harlow, Essex, UK;* [2]*Neurology and GI Centre of Excellence for Drug Discovery, GlaxoSmithKline, Harlow, Essex, UK;* [3]*MRC Centre for Synaptic Plasticity, Department of Anatomy, University of Bristol School of Medical Sciences, University Walk, Bristol, UK;* [4]*NeuroSolutions Ltd., Coventry, UK;* [5]*Psychiatry Centre of Excellence for Drug Discovery, GlaxoSmithKline, Verona, Italy;* [6]*School of Neurology, Neurobiology and Psychiatry, Newcastle University, Newcastle upon Tyne, UK and* [7]*Molecular Discovery Research, GlaxoSmithKline, Upper Providence, Collegeville, PA, USA*

Background and purpose: M_1 muscarinic ACh receptors (mAChRs) represent an attractive drug target for the treatment of cognitive deficits associated with diseases such as Alzheimer's disease and schizophrenia. However, the discovery of subtype-selective mAChR agonists has been hampered by the high degree of conservation of the orthosteric ACh-binding site among mAChR subtypes. The advent of functional screening assays has enabled the identification of agonists such as AC-42 (4-*n*-butyl-1-[4-(2-methylphenyl)-4-oxo-1-butyl]-piperidine), which bind to an allosteric site and selectively activate the M_1 mAChR subtype. However, studies with this compound have been limited to recombinantly expressed mAChRs.
Experimental approach: In this study, we have compared the pharmacological profile of AC-42 and a close structural analogue, 77-LH-28-1 (1-[3-(4-butyl-1-piperidinyl)propyl]-3,4-dihydro-2(1*H*)-quinolinone) at human recombinant, and rat native, mAChRs by calcium mobilization, inositol phosphate accumulation and both *in vitro* and *in vivo* electrophysiology.
Key results: Calcium mobilization and inositol phosphate accumulation assays revealed that both AC-42 and 77-LH-28-1 display high selectivity to activate the M_1 mAChR over other mAChR subtypes. Furthermore, 77-LH-28-1, but not AC-42, acted as an agonist at rat hippocampal M_1 receptors, as demonstrated by its ability to increase cell firing and initiate gamma frequency network oscillations. Finally, 77-LH-28-1 stimulated cell firing in the rat hippocampus *in vivo* following subcutaneous administration.
Conclusions and implications: These data suggest that 77-LH-28-1 is a potent, selective, bioavailable and brain-penetrant agonist at the M_1 mAChR and therefore that it represents a better tool than AC-42, with which to study the pharmacology of the M_1 mAChR.
British Journal of Pharmacology (2008) **154,** 1104–1115; doi:10.1038/bjp.2008.152; published online 5 May 2008

Keywords: muscarinic receptors; selective agonist; allosteric; AC-42; 77-LH-28-1; calcium mobilization; inositol phosphate; cell firing; network oscillations

Abbreviations: 77-LH-28-1, 1-[3-(4-butyl-1-piperidinyl)propyl]-3,4-dihydro-2(1*H*)-quinolinone; AC-42, 4-*n*-butyl-1-[4-(2-methylphenyl)-4-oxo-1-butyl]-piperidine; aCSF, artificial CSF; AUC, area under curve; CHO, Chinese hamster ovary; IP, inositol phosphate; mAChR, muscarinic ACh receptor; PSB, Pontamine Sky Blue; TM, transmembrane

Introduction

Muscarinic ACh receptors (mAChRs) are members of the rhodopsin-like G-protein-coupled receptor superfamily. There are five mAChR subtypes (M_1–M_5; Alexander *et al*, 2007): M_1, M_3 and M_5 receptor subtypes couple predominantly through $G_{q/11}$ proteins to mobilize intracellular calcium (Caulfield and Birdsall, 1998) and regulate multiple ion channel conductances, including the tonically active, voltage-dependent M current (Hamilton *et al*., 1997) as well as both N- and P/Q-type Ca^{2+} conductances (Shapiro *et al*., 1999). In contrast, M_2 and M_4 receptor subtypes couple predominantly through $G_{i/o}$ proteins to inhibit adenylyl cyclase and decrease intracellular cAMP levels (Caulfield and Birdsall, 1998).

Correspondence: Dr CJ Langmead, Neurophysiology & Pharmacology, Psychiatry CEDD, GlaxoSmithKline, Third Avenue, Harlow, Essex CM19 5AW, UK.
E-mail: christopher.j.langmead@gsk.com
Received 2 August 2007; revised 7 November 2007; accepted 1 April 2008; published online 5 May 2008

There is a wide array of pharmacological tools with which to study mAChRs. For example, *N*-methyl scopolamine, quinuclidinylbenzilate, pirenzepine and darifenacin are among numerous mAChR antagonists, and ACh and oxo-tremorine-M among mAChR agonists, which have been used in unlabelled and radiolabelled forms to characterize the localization, pharmacology and function of mAChRs. Unfortunately, most of these pharmacological tools exhibit poor selectivity between mAChR subtypes (Caulfield and Birdsall, 1998; Ellis, 2002). Those agents that do display high degrees of mAChR subtype selectivity are few in number and when discovered are often shown to interact with an allosteric, rather than the orthosteric, site as exemplified by the highly selective M_1 receptor peptide antagonist MT-7 (muscarinic toxin 7; Olianas *et al*., 2000).

Therefore, the identification of selective M_1 mAChR agonists would represent a significant advance in mAChR pharmacology and could offer the opportunity to validate the M_1 receptor as a drug target for the treatment of cognitive disorders. In this respect, Spalding *et al*. (2002) described a novel compound, AC-42, which activated the human recombinant M_1 mAChR but did not possess any significant agonist activity at the hM_2–hM_5 receptors. Functional studies using chimeric receptors indicated that the N-terminus–transmembrane (TM)1 and extracellular loop 3–TM7 regions of the M_1 receptor are required for selective activation by AC-42: regions that are distinct from the orthosteric site of the M_1 mAChR deeper in the TM bundle. Subsequently, it was demonstrated that AC-42 is an allosteric agonist of the M_1 mAChR (Langmead *et al*., 2006), a property that is likely to account for its good selectivity profile.

M_1 mAChRs are located centrally in regions such as the cortex, hippocampus and amygdala (Levey, 2003; Wess, 2003). This pattern of distribution suggests that this mAChR subtype may play a role in cognition. Indeed, certain molecules that are reported as being functionally selective M_1 mAChR agonists, such as xanomeline, sabcomeline and milameline, are effective in several preclinical models of cognition (Bodick *et al*., 1997; Harries *et al*., 1998; Dean *et al*., 2003; Weiner *et al*., 2004), although it must be noted that the absolute degree of selectivity of these molecules for M_1 receptors is dependent on the assay system used (Wood *et al*., 1999). In addition, there is early pre-clinical evidence to suggest that mAChR antagonists (Hagan *et al*., 1987) as well as lesioning of cholinergic projections in the forebrain of rats (Hagan *et al*., 1988; Smith, 1988) cause broad-ranging cognitive impairment. The latter evidence has been substantiated using more selective cholinergic lesioning methods such as the immunotoxin 192-IgG-saporin, which have clarified the interpretation of the earlier studies and substantiated the importance of the cholinergic system in attention (Maddux *et al*., 2007). Furthermore, in the M_1 mAChR knockout mouse, the induction of hippocampal long-term potentiation, synaptic plasticity, and learning and working memory are impaired (Anagnostaras *et al*., 2003; Wess, 2004; Shinoe *et al*., 2005). Therefore, M_1 mAChR activation offers a novel approach to potentially treat cognitive impairment in diseases such as Alzheimer's disease and, more recently, schizophrenia (Friedman, 2004). However, to date, the only clinical data generated from trials using the afore-mentioned functionally selective M_1 receptor agonists, xanomeline and milameline, have not robustly tested and proven the effectiveness of M_1 receptor agonism in the treatment of cognitive impairment (Bodick *et al*., 1997; Heidrich and Rösler, 1999). One reason for this may be that the therapeutic efficacy of these agents is hindered by dose-limiting side effects, including sweating, salivation, nausea and gastrointestinal disturbances, which is presumably due to their activation of other mAChR subtypes (Bodick *et al*., 1997; Heidrich and Rösler, 1999).

Despite the fact that AC-42 was the first M_1 mAChR allosteric agonist to be reported in the literature, the data published are limited to *in vitro* studies using human recombinant mAChRs. This present study compares the biological profile of AC-42 and a close structural analogue, 77-LH-28-1 (1-[3-(4-butyl-1-piperidinyl)propyl]-3,4-dihydro-2(1*H*)-quinolinone; Acadia patent WO2003/057672). *In vitro* calcium mobilization, inositol phosphate (IP) accumulation and electrophysiological assay systems were used to establish both the mAChR selectivity profile and the native tissue pharmacology of both AC-42 and 77-LH-28-1. Furthermore, *in vivo* pharmacokinetic and electrophysiological assays were undertaken to determine whether 77-LH-28-1 was brain penetrant and functionally active. To this end, our studies expand on and describe the *in vitro* and *in vivo* pharmacological profile that a selective, bioavailable M_1 mAChR agonist may offer.

Materials and methods

Animals

All animal procedures and *in vivo* studies conformed to GlaxoSmithKline ethical standards and were conducted in accordance with the United Kingdom Animals (Scientific Procedures) Act (1986).

Preparation of 77-LH-28-1

77-LH-28-1 was prepared as shown in Figure 1. Treatment of commercially available 3,4-dihydro-2(1*H*)-quinolinone (1) with 1-chloro-3-iodopropane and caesium carbonate in acetonitrile afforded the intermediate (2) in 54% yield. Reaction of (2) with 4-butylpiperidine in acetonitrile in the presence of potassium carbonate and sodium iodide resulted 77-LH-28-1 (3a;) as the free base in 29% yield. Conversion to the hydrochloride salt (3b) was accomplished by the treatment with hydrogen chloride in ether.

Cell culture

Chinese Hamster Ovary (CHO) cells stably expressing human M_1–M_5 mAChRs were obtained from National Institute of Mental Health (Bethesda, MD, USA; see Bonner, 1989). For calcium mobilization studies, CHO cell lines stably expressing human recombinant mAChRs (plus the chimeric G protein G_{qi5} for CHO-hM_2 and CHO-hM_4) were grown in Dulbecco's Modified Eagle's Medium (DMEM)/F12 medium plus 10% fetal bovine serum (FBS), 2 mM L-glutamine and

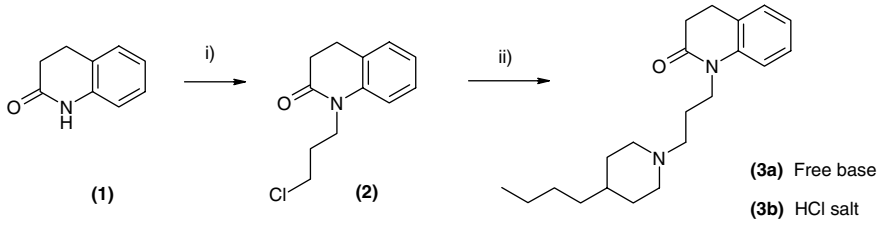

Figure 1 Preparation of 77-LH-28-1. 77-LH-28-1, 1-[3-(4-butyl-1-piperidinyl)propyl]-3,4-dihydro-2(1*H*)-quinolinone.

200 μg mL^{-1} G418. Cells were passaged twice weekly by treatment with Versene, centrifugation (200 *g*, 5 min) and re-suspension of the pellet in fresh media. CHO-hM_1 and CHO-hM_3 cells for IP-SPA (IP accumulation scintillation proximity assays) were routinely cultured in Alpha minimum essential medium (MEM) with ribonucleosides plus 10% FBS. Cells were maintained in a humidified atmosphere at 37 °C in 5% CO_2 and passaged twice weekly by scraping in media, centrifugation (200 *g*, 5 min) and re-suspension of the pellet in fresh media.

CHO-hM_1–hM_5 calcium mobilization assays

Briefly, 20 000 cells per well were seeded in 384-well Greiner Bio-One plates in culture medium (DMEM with 10% FBS), incubated overnight in a humidified atmosphere at 37 °C in 5% CO_2. After aspirating the medium, cells were loaded with the cytoplasmic calcium indicator Calcium 3 dye (Molecular Devices, Sunnyvale, CA, USA; 30 μL per well in Hank's balanced salts with 20 mM HEPES) and incubated in a humidified atmosphere at 37 °C in 5% CO_2 for 60 min. Assay buffer (Hank's balanced salts with 20 mM HEPES; 10 μL per well) containing different concentrations of compounds was then added to the cells on a fluorometric imaging plate reader (Molecular Devices). The increase in intracellular calcium induced by compounds of interest was recorded as a change in the fluorescent signal. pEC_{50} values for each compound were determined by an 11-point dilution concentration–response curve spanning a 5.5 log unit concentration range. In situations where robust agonist activity was not observed at concentrations up to 10 μM, compounds were preincubated with cells for 30 min and tested for antagonism of the calcium mobilization responses induced by an EC_{80} concentration of ACh (4–8 nM).

IP accumulation scintillation proximity assay

IP-SPAs were performed as described in Brandish *et al*. (2003) with minor modifications. CHO-hM_1 or CHO-hM_3 cells were seeded into clear bottomed, black-walled 96-well microtitre plates (Fisher Scientific, Loughborough, UK) at a density of 50 000 cells per well. After 24 h, the cell medium was removed and replaced with 100 μL inositol-free DMEM containing 10 μCi mL^{-1} [^{3}H]-*myo*-inositol (Amersham Biosciences, Little Chalfont, UK). After 16 h, the [^{3}H]-*myo*-inositol was removed and the cells were washed with 2 × 200 μL inositol-free DMEM. For antagonist assays, cells were then incubated with 100 μL antagonist in inositol-free DMEM containing 5 mM LiCl for 30 min prior to the addition of 100 μL agonist. IP accumulation was allowed to continue for 1 h at 37 °C after which the reaction was terminated by the removal of the medium and the addition of 200 μL 0.1 M formic acid (Sigma-Aldrich, Poole, UK) to extract IP. The extraction was allowed to continue for 1 h at room temperature after which 20 μL samples of the extracts were removed from each well and combined with 80 μL of RNA-binding yttrium silicate SPA beads (12.5 mg mL^{-1}) in opaque-bottomed 96-well picoplates (Perkin Elmer, Seer Green, UK). Plates were agitated for 1 h at room temperature and the beads left to settle for 2 h. Total inositol phosphate ([^{3}H]IP_X) accumulation (c.p.m.) for each concentration of agonist was determined on a TopCount plate counter (Perkin Elmer). Agonist concentration–response curves were analysed using a four-parameter logistic fit; pirenzepine and scopolamine datasets were analysed according to models of both competitive and allosteric interactions (Langmead *et al*., 2006; Prism 4, GraphPad).

Rat hippocampal CA1 cell firing studies

Rats (Sprague–Dawley, Charles River, Margate, UK; 180–230 g) were killed and 400 μm sagittal brain slices containing the hippocampus were prepared. The hippocampal CA3 region of each slice was removed and the remaining slice transferred to a recording chamber. Slices were perfused at 4 mL min^{-1} with artificial CSF (aCSF) (in mM: 124 NaCl, 5 KCl, 26 $NaHCO_3$, 1.2 Na_2HPO_4, 1.3 $MgCl_2$, 2.4 $CaCl_2$, 10 glucose) bubbled with 95% O_2/5% CO_2 and maintained at 32–34 °C. Recording electrodes were pulled on a DMZ Universal Puller from borosilicate glass capillaries (Clark Electromedical Instruments, Reading, UK—GF120TF-10) and filled with aCSF. Tip diameter was >2 μm and resistance was <5 MΩ. Electrodes were positioned in the pyramidal cell layer of the CA1 region under microscopic control using PatchStar manipulators (Scientifica, Uckfield, UK) until a dominant signal could be readily distinguished above the

background noise. The initial search for activity was performed in the presence of 1 μM carbachol. In each slice, once single or multiple units were identified, carbachol was washed out and 1 μM carbachol re-applied to allow normalization of data across experiments. Recorded signals were amplified 10 000 times using an AxoClamp 2B amplifier (Molecular Devices), in series with a secondary amplifier (Brownlee Precision Instruments, San Jose, CA, USA). Signals were band pass filtered between 0.1 and 3 kHz, digitized at 10 kHz (Digidata 1332, Molecular Devices) and captured using Clampex 9.2 (Molecular Devices) and stored in a PC for off-line analysis. Electrical noise (50 Hz) was removed with a Humbug (Quest Scientific, North Vancouver, BC, Canada). Drugs were bath-applied for 10–20 min until a steady-state effect was reached. Cumulative concentration–response curves for AC-42 and 77-LH-28-1 were constructed in 0.5 log molar increments. Where pirenzepine was used, it was pre-applied for 30 min prior to the agonist.

Extracellular recordings of action potentials were analysed using the spike sorting feature of Spike2 (Cambridge Electronic Design, Cambridge, UK). The effect of a given test compound was evaluated by measuring the mean discharge frequency during the final 2 min of exposure to each concentration of drug. Neuronal firing frequency in the presence of drug was expressed as a ratio of a reference 1 μM carbachol response in each slice. Concentration–response curves were fitted and pEC_{50} values calculated using GraFit 5.0 (Erithacus Software, Horley, UK). The intrinsic activity of a compound was calculated as the ratio of the maximum response to the drug/the maximum response to carbachol, both derived from the curve fits to the respective mean data. Data are the mean of $n=3$ (77-LH-28-1 alone), $n=5$ (carbachol plus pirenzepine) or $n=13$ (carbachol alone) independent experiments with 1 or 2 separate '*n*'-values per animal.

Whole-cell patch-clamp electrophysiology in rat hippocampus

Brains from P13–15 male Wistar rat pups were dissected after a lethal dose of anaesthetic (pentobarbitone) and decapitation, and placed in ice-cold aCSF (119 mM NaCl, 2.5 mM KCl, 1 mM $NaH_2PO_4 \cdot H_2O$, 26.2 mM $NaHCO_3$, 1 mM glucose, 2.5 mM $CaCl_2$ and 1.3 mM $MgSO_4$) gassed with 95% O_2 and 5% CO_2. A 300 μm measurement of transverse hippocampal slices was cut using a vibrotome (DTK-1000; DSK, Osaka, Japan). Slices were then incubated at 36 °C for 30 min and rested at room temperature for a further 30 min. The connections between CA3 and CA1 region were severed using a scalpel to prevent recurrent excitatory input. Slices were then transferred to a submersion recording chamber at 32 °C and superfused with the extracellular solution described above supplemented with 50 μM picrotoxin to block $GABA_A$ receptors.

Neurons in the stratum pyramidale were visualized using standard infrared differential interference contrast microscopy. Patch pipettes of resistance 3–6 MΩ were filled with an intracellular solution consisting of 120 mM $KMeSO_3$, 10 mM HEPES, 0.2 mM EGTA, 4 mM Mg-ATP, 0.3 mM Na-GTP, 10 mM KCl, 8 mM NaCl, pH 7.5 and 280 mosM. Whole-cell current-clamp recordings were made from CA1 pyramidal cells at 32 °C using a Multiclamp 700A amplifier (Axon Instruments, Sunnyvale, CA, USA). Membrane potential and input resistance were monitored until 20 min of stable baseline had been achieved. Compounds were then added to the perfusing aCSF and monitoring of membrane potential and input resistance continued. All data were corrected for a calculated liquid junction potential of 9 mV.

Network oscillations in rat hippocampus

Horizontal hippocampal slices were prepared from male Lister hooded rats aged between 4 and 6 weeks as described previously (Brown *et al*., 2006). After dissection, slices were transferred to an interface-style recording chamber maintained at 32 ± 1 °C, humidified with 95% O_2/5% CO_2 and perfused (2–3 mL min^{-1}) with aCSF comprising (in mM) 124 NaCl, 3 KCl, 26 $NaHCO_3$, 2 $CaCl_2$, 1.25 NaH_2PO_4, 1 $MgSO_4$, 10 D-glucose. Extracellular field recordings were made using glass micropipettes (2–4 MΩ) filled with aCSF and placed in the stratum pyramidale of CA3 area. Correct positioning of the recording electrode was confirmed by electrical stimulation of the mossy fibre pathway using a concentric bipolar stimulating electrode (inner diameter 12.5 μm; FHC Inc., Bowdoinham, ME, USA), connected to an isolated stimulator box, positioned in the dentate hilus. Gamma frequency oscillations were evoked by the addition of 77-LH-28-1 to the perfusion medium. Recorded signals were amplified 2000 times using an AxoClamp 2B amplifier (Molecular Devices), in series with a secondary amplifier (Brownlee Precision Instruments). Signals were then band pass filtered between 0.1 and 3 kHz, digitized at 10 kHz, captured using Clampex 9.2 (Molecular Devices) and stored in a PC hard disc for off-line analysis. Any additional filtering was performed digitally on pre-recorded data. Clampfit 9.2 software (Molecular Devices) was used to perform fast Fourier transforms. The data presented are mean ± s.e.mean. The '*n*'-values represent the number of times an experiment was performed, each in a different slice (1 or 2 separate '*n*'-values per animal).

Pharmacokinetics of 77-LH-28-1 after intraperitoneal and subcutaneous administration to the rat

Prior to commencing any *in vivo* studies with 77-LH-28-1, studies were performed to determine the pharmacokinetics and brain penetration of 77-LH-28-1 in the male rat after intraperitoneal and subcutaneous administration. For intraperitoneal administration, 77-LH-28-1 was suspended in 1% (w/v) methylcellulose in water and for subcutaneous administration 77-LH-28-1 was dissolved in normal saline. For both intraperitoneal and subcutaneous routes of administration, 77-LH-28-1 was administered to six male Sprague–Dawley rats at a dose of 3 mg kg^{-1}. Individual animals were killed at 0.25, 0.5, 1, 2, 3 and 5 h after each dose administration, and blood and brains collected and frozen (approximately −80 °C) prior to analysis.

Preparation and analysis of blood samples

Blood aliquots (100 μL) were prepared for analysis by extracting with 300 μL of the protein precipitation solvent

(95:5 acetonitrile/ethanol, containing 0.1% (v/v) formic acid and 10 ng mL^{-1} internal standard), mixed and centrifuged at 1500 *g* for 15 min. Aliquots of the supernatant (100 μL) were diluted 1:1 (v/v) with water and analysed using a specific HPLC-MS/MS assay (Waters Quattro premier mass spectrometer). Concentrations of 77-LH-28-1 were determined using calibration standards prepared in the same manner with a range of 0.5–2000 ng mL^{-1}.

Preparation and analysis of brain samples
Each excised brain was thawed, weighed and to each gram of brain 2.15 mL methanol/water (1:1; v/v) was added. Each brain was homogenized using an autogizer (Tomtec, Hamden, CT, USA). Aliquots (200 μL) of homogenized brain were extracted with 400 μL protein precipitation solvent, as described in the blood analysis. Aliquots of the resulting supernatant (100 μL) were removed and diluted with water (1:1; v/v) and analysed using a specific HPLC-MS/MS assay (Waters Quattro premier mass spectrometer). Concentrations of 77-LH-28-1 were determined using calibration standards prepared in the same manner with a range of 1.5–3000 ng g^{-1}.

Neuronal activity in the CA1 region of rat hippocampus: in vivo *electrophysiology*
Male Sprague–Dawley rats (270–370 g; B&K Scientific, Grimston, UK) were anaesthetized with urethane, and the right femoral artery was cannulated for the recording of arterial blood pressure via a pressure amplifier (Neurolog, NL108). Urethane was administered by intraperitoneal injection of a 12% solution (10 mL kg^{-1}). Additional anaesthetic was administered when required (2 mL kg^{-1}), assessed by cardiovascular responses to paw-pinch and the stability of measured cardiovascular variables.

Animals were divided into three groups of which one received 3 mg kg^{-1} 77-LH-28-1 subcutaneously ($n=3$), another group received volume-matched saline vehicle subcutaneously ($n=3$) and the final group received scopolamine (3 mg kg^{-1}, i.p.) 15 min before subcutaneous administration of 3 mg kg^{-1} 77-LH-28-1 ($n=3$). The testing of vehicle, compound and scopolamine pretreatment was randomized, and no significant differences in blood pressure recordings were found between the treatment groups.

After anaesthesia, the trachea was exposed and cannulated, and animals were allowed to breathe room air, which in some cases was oxygen-enriched. The skull bone was removed at the following stereotaxic coordinates; 3–5 mm caudal to bregma and 1.5–3.5 mm lateral to the midline. The dural layers overlying the brain were subsequently cut and reflected laterally allowing for the removal of the pia matter directly adjacent to the track of electrode descent. Electrodes were descended through the cortex using a single-axis hydraulic micromanipulator (Narishige, MO-15S) to the hippocampus where CA1 pyramidal neurons were located and identified by their stereotaxic coordinates; bregma −4.2, lateral 2.4, 1.8–2.4 mm below pial surface (Paxinos and Watson, 1986) and by the location of marked recording sites (see below).

Extracellular recordings were made from hippocampal neurons using multibarrelled (4) glass microelectrodes purchased from Kation Scientific (Minneapolis, MN, USA) using a carbon fibre for the recording of neuronal activity (Carbostar-4; impedance at 1 kHz, carbon fibre: 0.4–0.8 MΩ, pipettes 8–10 MΩ (when filled with 200 mM NaCl)). Pipette barrels contained Pontamine Sky Blue (PSB, 2% dissolved in 0.5 M sodium acetate) and the glutamate receptor agonist DL-homocysteic acid. These compounds were ejected via iontophoresis (Neurophore, Medical Systems, Welwyn Garden City, UK) with the PSB solution-containing barrel providing the balancing for this current ejection. In some experiments, a low current of DL-homocysteic acid (0–10 nA) was continuously ejected iontophoretically while searching for and testing neuronal activity. This provided an excitatory drive for cells with no spontaneous activity, aiding both their identification and the characterization of the effects of test compounds on these neurons. Neuronal activity was recorded using a Neurolog headstage (model NL105), connected to a Neurolog amplifier (×10 000; Neurolog AC preamplifier NL104) and filter (0.5–5 kHz; Neurolog filter, model NL125), the subsequent output was transmitted to the PC via the micro 1401 interface (Cambridge Electronic Design). This activity was discriminated and counted using a window discriminator (Digitimer, Welwyn Garden City, UK; model D130), and, using Spike2 software (Cambridge Electronic Design) was presented as a rate histogram with units of spikes per bin.

In all experiments, PSB was injected via iontophoresis into the hippocampus after the termination of neuronal recording for the identification and localization of recorded cells. At the end of the experiment, the marked brains were removed, hemisected and snap-frozen over dry ice. Serial cryosectioning (at a thickness of 30 μm) of the hemisphere in which recording was carried out and PSB marked recording sites were then visualized under a light microscope and mapped onto a standard stereotaxic atlas of the appropriate region of the rat hippocampus confirming the location of specific recording sites (Figures 8b and c).

Neuronal activity was analysed in bins of 5 min and a stable 5-min period of baseline activity was recorded before test compounds were administered. All analysis was performed using Spike2 software and online scripts available from http://www.ced.co.uk. All post-dose neuronal activity was normalized to baseline activity before calculating mean values.

Materials
All cell culture reagents were purchased from Invitrogen (Paisley, UK). [^{3}H]-*myo*-inositol was purchased from Amersham Biosciences. All other chemicals were purchased from Sigma-Aldrich or BDH (Poole, UK).

Results

Calcium mobilization studies
Calcium mobilization studies were carried out to determine the ability of AC-42 and 77-LH-28-1 to selectively activate M_1 receptors over the other mAChR subtypes. Both AC-42 and 77-LH-28-1 potently stimulated intracellular calcium

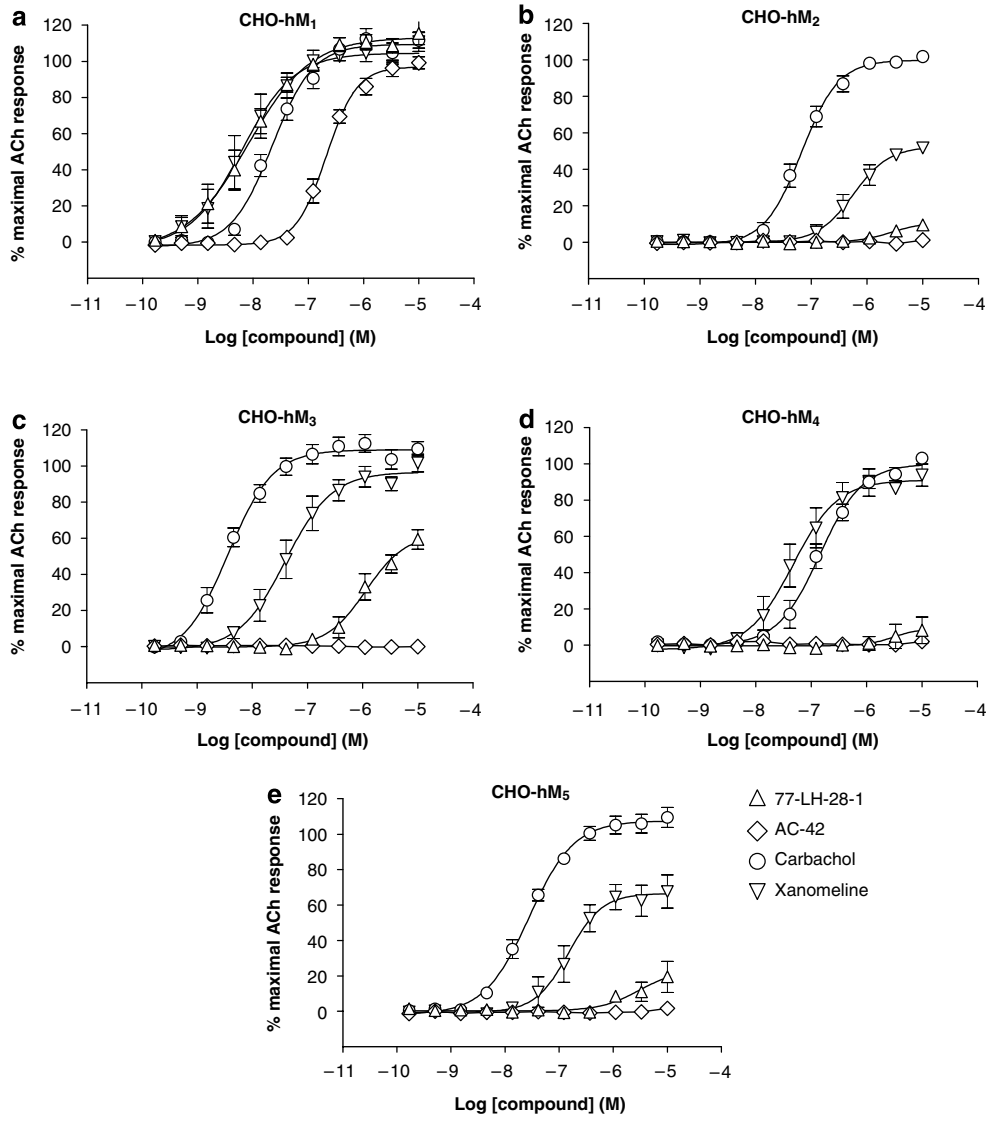

Figure 2 (**a**–**e**) Concentration-dependent stimulation of intracellular calcium mobilization in CHO-hM_1–hM_5 cells by carbachol, xanomeline, AC-42 and 77-LH-28-1. Data are the mean of at least four independent experiments (±s.e.mean). 77-LH-28-1, 1-[3-(4-butyl-1-piperidinyl)propyl]-3,4-dihydro-2(1*H*)-quinolinone.

Table 1 pEC_{50} values (±s.e.mean) for intracellular Ca^{2+} mobilization induced by carbachol, xanomeline and 77-LH-28-1 in CHO cells stably expressing human M_1–M_5 mAChR subtypes (along with $G\alpha_{qi5}$ for M_2 and M_4 receptor subtypes)

	CHO-hM1	*CHO-hM2*	*CHO-hM3*	*CHO-hM4*	*CHO-hM5*
Carbachol, pEC_{50}	7.6±0.1 (98±1)	7.1±0.1 (98±1)	8.3±0.1 (98±1)	6.9±0.1 (105±1)	8.2±0.1 (99±1)
Xanomeline, pEC_{50}	7.7±0.1 (95±1)	6.0±0.1 (64±1)	7.1±0.1 (80±1)	7.4±0.1 (90±1)	6.7±0.1 (74±1)
77-LH-28-1, pEC_{50}	8.1±0.3 (103±3)	<5	5.6±0.2 (65±5)	<5	<5
77-LH-28-1, pIC_{50}	—	5.5±0.1	—	5.9±0.2	5.8±0.4
AC-42, pEC_{50}	6.5±0.1 (97±1)	<5	<5	<5	<5
AC-42, pIC_{50}	—	5.1±0.1	5.0±0.1	5.1±0.1	<5

Abbreviations: 77-LH-28-1, 1-[3-(4-butyl-1-piperidinyl)propyl]-3,4-dihydro-2(1*H*)-quinolinone; AC-42, 4-n-butyl-1-[4-(2-methylphenyl)-4-oxo-1-butyl]-piperidine; CHO, Chinese Hamster Ovary cells; mAChR, muscarinic ACh receptor.
Percentage efficacy (±s.e.mean; with respect to the maximal asymptotic response to ACh) is shown in parentheses. Where no robust agonist activity could be detected for 77-LH-28-1, pIC_{50} values (±s.e.mean) to inhibit Ca^{2+} mobilization induced by an EC_{80} concentration of ACh (4–8 nM) are quoted. Data represent the mean (±s.e.mean) of at least four independent experiments.

mobilization in CHO-hM_1 cells with pEC_{50} values of 6.5±0.1 and 8.1±0.3, respectively (Figure 2; Table 1). As shown previously, AC-42 does not display agonist activity at hM_2–hM_5 receptor subtypes at concentrations up to 10 μM (Table 1; Figure 2; Spalding *et al.*, 2002) and displays only weak antagonist activity at hM_2, hM_3 and hM_4 receptor

subtypes. 77-LH-28-1 only weakly stimulated calcium mobilization in CHO-hM_3 cells with a pEC_{50} value of 5.6 ± 0.2 with little or no agonist activity up to 10 μM at the hM_2, hM_4 and hM_5 receptor subtypes (Figure 2; Table 1).

Additionally, 77-LH-28-1 displayed only weak antagonist affinity at these receptor subtypes, with pIC_{50} values for inhibition of ACh-stimulated calcium mobilization being less than 6 (Table 1). This selective profile of hM_1 mAChR activation contrasts markedly with the broad-spectrum mAChR agonist profile displayed by both carbachol and xanomeline (Figure 2; Table 1).

Accumulation of IP in CHO cells

Accumulation of IP was studied in CHO cells with recombinantly expressed hM_1 and hM_3 receptors to determine whether the selectivity profile of AC-42 and 77-LH-28-1 observed in the calcium mobilization assay was maintained in a different assay system. Carbachol, AC-42 and 77-LH-28-1 all stimulated IP accumulation in CHO-hM_1 cells, with pEC_{50} values of 6.35 ± 0.02, 6.21 ± 0.10 and 7.37 ± 0.09, respectively, with AC-42 (0.85) and 77-LH-28-1 (0.95) displaying high intrinsic activity with respect to the full agonist carbachol (Figure 3a). Although carbachol also caused a robust stimulation of IP accumulation in CHO-hM_3 cells ($pEC_{50} = 6.81 \pm 0.04$), neither AC-42 nor 77-LH-28-1 exhibited any appreciable agonist activity at this mAChR subtype at concentrations up to 100 μM (Figure 3a), suggesting that the selective M_1 mAChR agonist profile of AC-42 and 77-LH-28-1 observed in the calcium mobilization assay is maintained in an IP assay system.

To validate the experimental design of the subsequent electrophysiology studies, the ability of the mAChR antagonists pirenzepine and scopolamine to antagonize 77-LH-28-1-stimulated IP accumulation was also investigated. Both pirenzepine and scopolamine caused a concentration-dependent rightward shift in the concentration–response curve to 77-LH-28-1, with no depression in the maximal response (Figures 3b and c). Comparison of the analysis of the datasets according to the models of competitive antagonism and allosteric interaction (Langmead *et al*., 2006) failed to distinguish between the two potential mechanisms of action. Accordingly, the data were analysed according the former, simpler model, yielding estimates of pK_B values of 8.0 ± 0.2 and 9.5 ± 0.2 for pirenzepine and scopolamine, respectively. These data suggest that both pirenzepine and scopolamine are suitable tools with which to block the effects of 77-LH-28-1 at the M_1 mAChR.

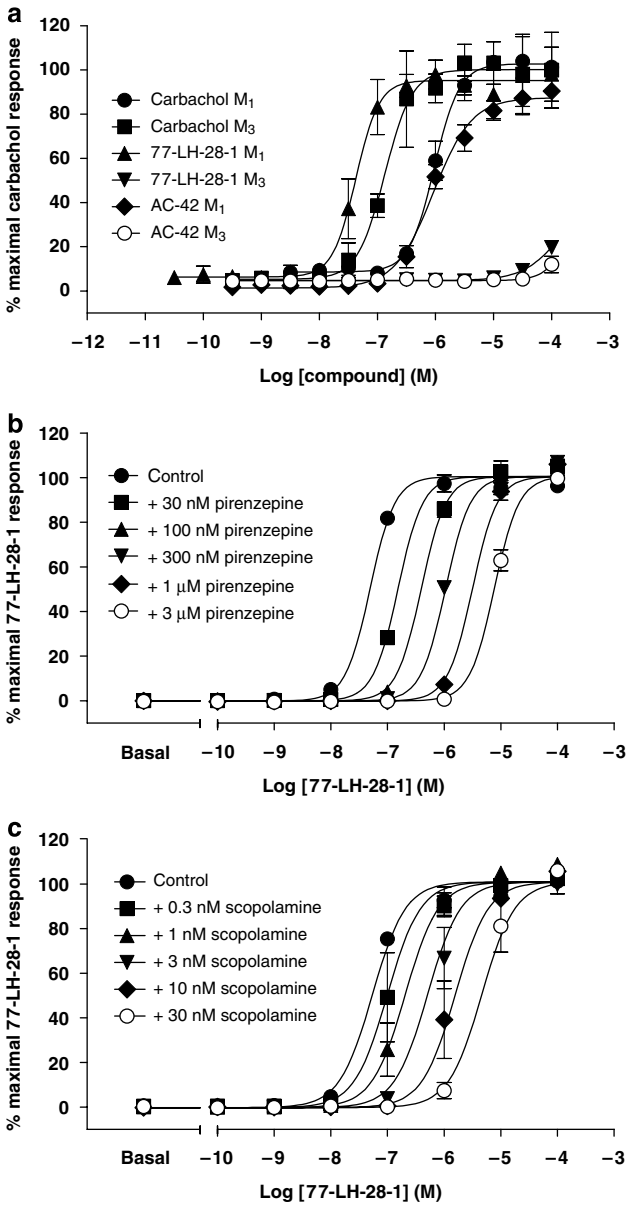

Figure 3 (**a**) Concentration-dependent stimulation of IP accumulation in CHO-hM_1 and CHO-hM_3 cells by carbachol, AC-42 and 77-LH-28-1, and the effect of mAChR antagonists pirenzepine (**b**) and scopolamine (**c**) on the 77-LH-28-1 response in CHO-hM_1 cells. Data are the mean of at least three independent experiments (± s.e.mean). 77-LH-28-1, 1-[3-(4-butyl-1-piperidinyl)propyl]-3,4-dihydro-2(1*H*)-quinolinone; AC-42, 4-*n*-butyl-1-[4-(2-methylphenyl)-4-oxo-1-butyl]-piperidine; CHO, Chinese Hamster Ovary cells.

Rat hippocampus CA1 cell firing in vitro

Although compounds such as AC-42 and 77-LH-28-1 have been shown to selectively activate the M_1 mAChR subtype in recombinant systems, it is unclear whether they are able to drive M_1 mAChR activation in native tissue systems. Therefore, both AC-42 and 77-LH-28-1 were assessed for their ability to initiate single-unit cell firing in the CA1 region of the rat hippocampus. In this brain region, carbachol stimulated cell firing with a pEC_{50} value of 5.7 ($n = 13$; Figure 4a). The application of the M_1 mAChR-preferring antagonist pirenzepine (100 nM) caused a parallel rightward shift in the carbachol concentration–response curve with no depression in the maximal response (Figure 4a), with a calculated pA_2 value of 7.7, suggesting that carbachol mediated its response, predominantly, via the activation of the M_1 mAChR subtype (Dorje *et al*., 1990). AC-42, at concentrations up to 30 μM, failed to significantly stimulate cell firing (Figure 4b). In contrast, 77-LH-28-1 stimulated single-unit firing, acting as a full agonist with respect to carbachol, with a pEC_{50} value of 6.3 ($n = 3$; Figure 4b).

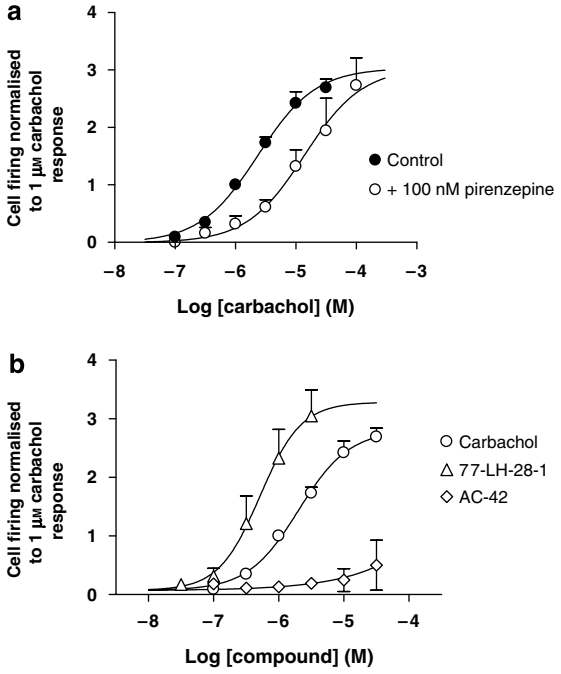

Figure 4 (**a**) Antagonism of carbachol-stimulated cell firing in the CA1 region of the rat hippocampus by pirenzepine and (**b**) effect of 77-LH-28-1 on cell firing in the CA1 region of the rat hippocampus. 77-LH-28-1, 1-[3-(4-butyl-1-piperidinyl)propyl]-3,4-dihydro-2(1*H*)-quinolinone.

Whole-cell patch-clamp analysis of rat hippocampal CA1 pyramidal neurons

The increase in single-unit firing by 77-LH-28-1 described above could result from either a direct action on the pyramidal cells or an increase in excitability mediated indirectly through changes in synaptic activity. To investigate this further, whole-cell patch-clamp recordings were made from individual CA1 pyramidal neurons. In all cells tested, 77-LH-28-1 (10 μM) depolarized the membrane potential producing a mean peak depolarization of 8.2 ± 1.2 mV ($n = 5$, Figure 5a). This depolarization was sustained with no evidence of tachyphalaxis on prolonged application of 77-LH-28-1. A 45 ± 13% increase in input resistance from 128 ± 14 to 168 ± 14 MΩ was associated with this depolarization (Figure 5b) and both effects were almost eliminated by prior application of pirenzepine (3 μM, $n = 6$, Figure 5c).

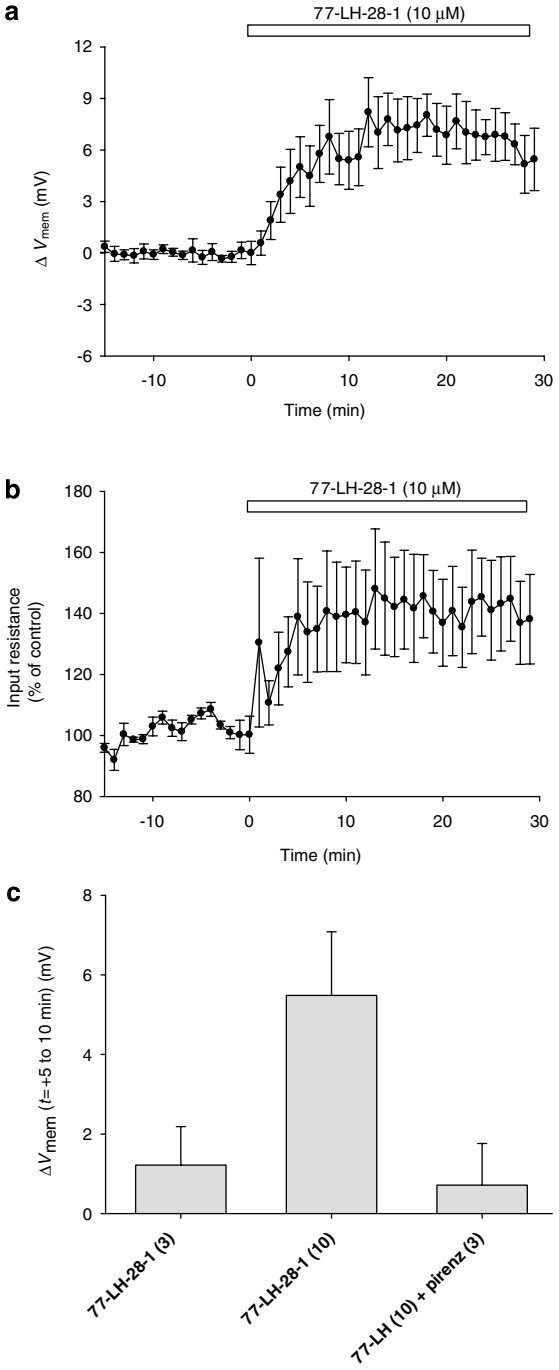

Figure 5 Depolarization of CA1 pyramidal cells by 77-LH-28-1. (**a**) Mean time course of the membrane potential of five pyramidal cell exposed to 10 μM 77-LH-28-1 at time = 0. The membrane potential is expressed relative to the mean of the baseline period (−69.0 ± 3.6 mV for these cells). (**b**) A plot of the input resistance (expressed as percent of baseline) for the same five cells. (**c**) Summary data plotting the mean depolarization observed after 5–10 min of application of 77-LH-28-1 at 3 μM ($n = 5$) and 10 μM ($n = 5$), and 10 μM 77-LH-28-1 in the presence of 3 μM pirenzepine ($n = 6$). 77-LH-28-1, 1-[3-(4-butyl-1-piperidinyl)propyl]-3,4-dihydro-2(1*H*)-quinolinone.

Rat hippocampal network oscillations

Agents that depolarize hippocampal neurons can produce synchronous network activity in the gamma and/or theta frequency bands. Indeed, mAChR activation has been shown to induce gamma oscillations (Fisahn *et al*., 1998), and knockout mouse studies have implicated the M_1 mAChR receptor subtype as playing a major role in the initiation of such network activity (Fisahn *et al*., 2002). We therefore tested whether 77-LH-28-1 would initiate network oscillations in the rat hippocampus *in vitro*. Carbachol (10 μM) induced gamma frequency oscillations in the CA3 region that exhibited a mean frequency of 30.5 ± 0.5 Hz and power of 3.94 ± 0.56 μV^2 ($n = 5$; data not shown). 77-LH-28-1 (10 μM) also induced gamma frequency (30–80 Hz) oscillations in this brain region displaying a frequency of 35.0 ± 1.0 Hz (Figure 6a) and power (described by the

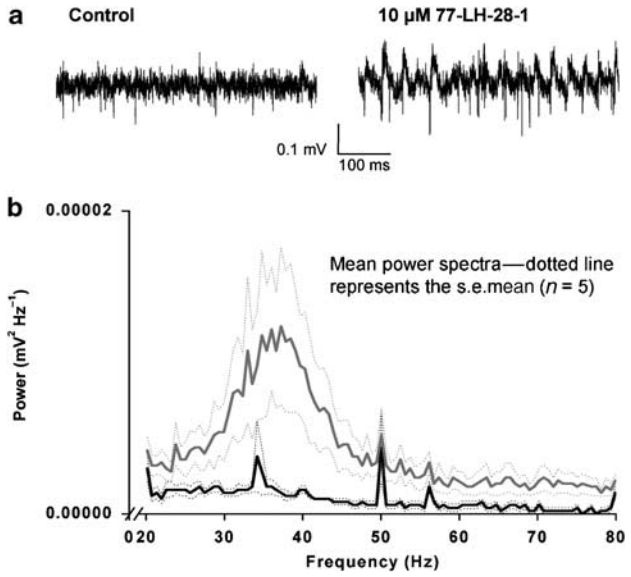

Figure 6 (**a**) Recording of extracellular activity for 500 ms from the CA3 region of the rat hippocampus during control conditions and after the addition of 77-LH-28-1 (10 μM). (**b**) Power spectra from a 60-s epoch of extracellular activity (control response shown in black; 77-LH-28-1 (10 μM) is shown in red). Dotted line represents the s.e.mean. 1-[3-(4-butyl-1-piperidinyl)propyl]-3,4-dihydro-2(1*H*)-quinolinone.

area under the curve over the 30–80 Hz range) of $0.015 \pm 0.006\,\mu V^2$ ($n = 5$; Figure 6b).

Pharmacokinetics of 77-LH-28-1 after intraperitoneal and subcutaneous administration to the rat

The blood and brain concentration–time profiles in the male rat after intraperitoneal and subcutaneous administration of 77-LH-28-1 at $3\,mg\,kg^{-1}$ are shown in Figure 7. Blood concentrations of 77-LH-28-1 after subcutaneous administration were greater than those obtained after intraperitoneal administration, and therefore the subcutaneous route represents a more viable route of administration for investigating the *in vivo* activity of 77-LH-28-1.

After subcutaneous administration, 77-LH-28-1 was rapidly absorbed with T_{max} occurring at the first measurable time point (0.25 h). Blood C_{max} was equivalent to $759\,ng\,mL^{-1}$ with concentrations declining rapidly and was equivalent to $151\,ng\,mL^{-1}$ at 0.5 h. Brain concentrations of 77-LH-28-1 were greater than those in blood resulting in a brain/blood AUC ratio of approximately 4:1.

Rat hippocampus CA1 cell firing in vivo

To verify whether *in vitro* activation of rat native M_1 mAChRs by 77-LH-28-1 would result in the activation of rat hippocampal CA1 neurons *in vivo*, an electrophysiology study was performed. As expected, administration of 77-LH-28-1 ($3\,mg\,kg^{-1}$, s.c.) enhanced neuronal activity (ongoing and evoked) in the CA1 region of the rat hippocampus (Figure 8; $P<0.01$, repeated measures ANOVA). A maximal increase in cell firing was observed after 30–35 min ($351 \pm 67.5\%$ of baseline activity), although there was a

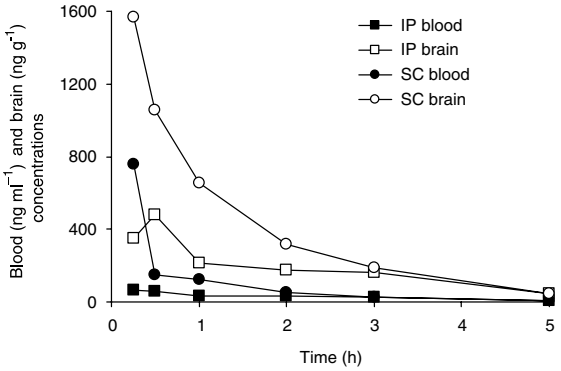

Figure 7 Blood and brain concentration–time profiles for 77-LH-28-1 after intraperitoneal (i.p.) and subcutaneous (s.c.) administration of 77-LH-28-1 to the male Sprague–Dawley rat at $3\,mg\,kg^{-1}$. 77-LH-28-1, 1-[3-(4-butyl-1-piperidinyl)propyl]-3,4-dihydro-2(1*H*)-quinolinone.

partial waning of this response to $257 \pm 34.2\%$ of baseline activity 55 min after administration. Pretreatment with the broad-spectrum mAChR antagonist scopolamine ($3\,mg\,kg^{-1}$, i.p.) attenuated the enhancement of neuronal activity induced by 77-LH-28-1 to $95 \pm 33.8\%$ of baseline activity 30–35 min after 77-LH-28-1 administration (Figure 8). Notably, there was no effect of vehicle (saline, s.c.) on neuronal activity.

Discussion

Recently, M_1 mAChR agonism has been implicated in the treatment of the cognitive impairment associated with both Alzheimer's disease and schizophrenia (Cortes *et al*., 1987; Friedman, 2004). The mAChR agonists developed to date, such as xanomeline and sabcomeline, improve cognition preclinically, although evidence of clinical efficacy has been confounded by peripheral effects such as sweating, nausea and diarrhoea, which are believed to be attributed to the relatively non-selective mAChR activity profile of these compounds (Wood *et al*., 1999). This lack of selectivity is believed to be due to binding to the orthosteric ACh binding site that is highly conserved across the mAChR family (Spalding *et al*., 1994; Baldwin *et al*., 1997; Gether, 2000; Lu *et al*, 2001).

The discovery of AC-42 as a selective, allosteric agonist of the M_1 mAChR (Spalding *et al*., 2002; Langmead *et al*., 2006), has opened up the possibility of designing agonists that display true selectivity over M_2–M_5 mAChRs. However, studies to date with this compound have been limited to recombinantly expressed mAChRs. To this end, we have synthesized and carried out a series of pharmacological assays to elucidate the *in vitro* and *in vivo* profile of 77-LH-28-1 and compared it to the profile of AC-42 to establish whether this molecule provides a better M_1 mAChR agonist with which to evaluate the role of native M_1 receptors *in vitro* and *in vivo*.

Calcium mobilization studies demonstrated that AC-42 and 77-LH-28-1 displayed functional selectivity for M_1

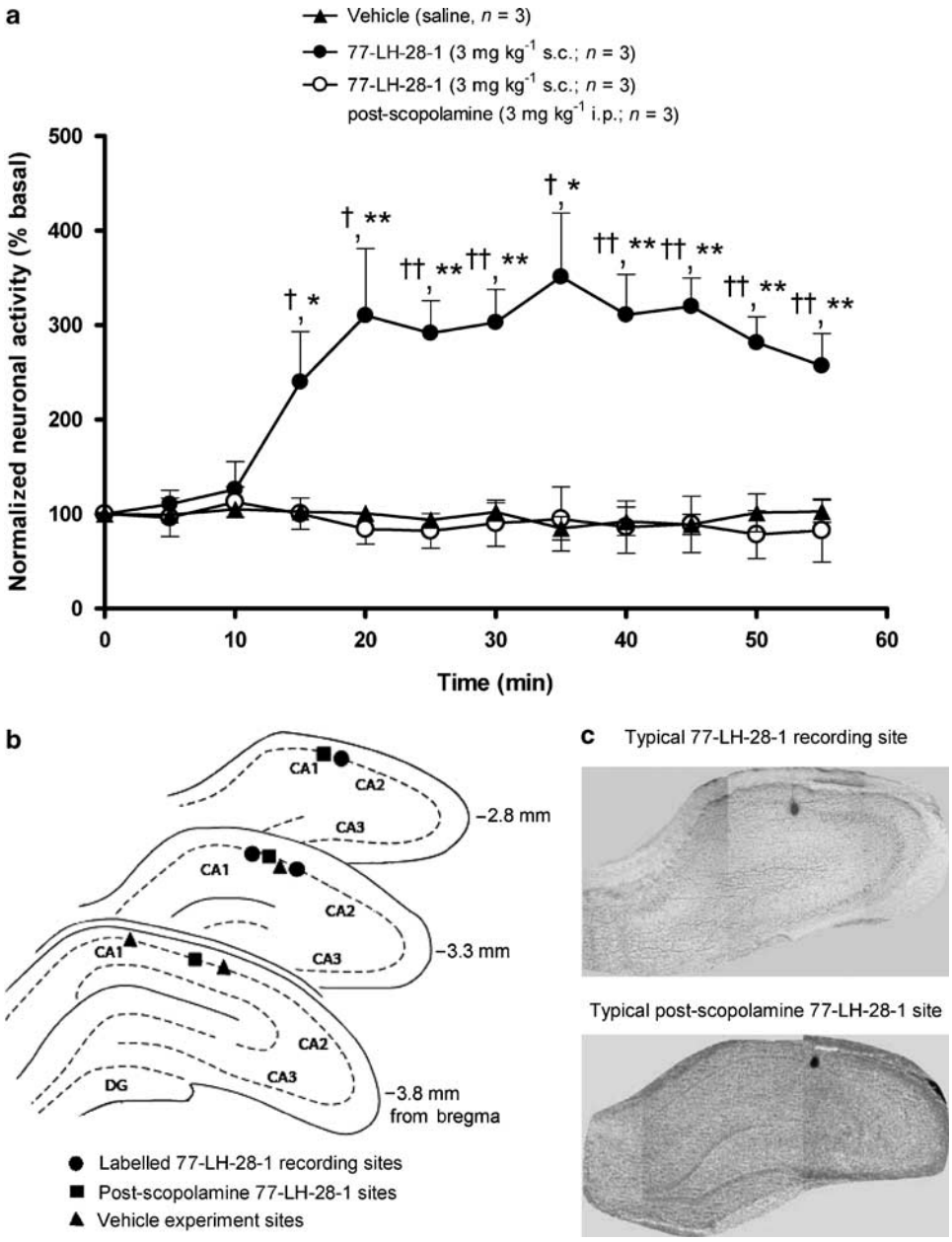

Figure 8 (**a**) 77-LH-28-1 enhances neuronal activity in the CA1 region of the rat hippocampus. Normalized neuronal activity plotted against time. $^{*}P<0.05$; $^{**}P<0.01$ vs 77-LH-28-1 and scopolamine (Fisher LSD test). $^{\dagger}P<0.05$; $^{\dagger\dagger}P<0.01$ vs vehicle using Fisher least significant difference test; vertical bars represent s.e.mean. (**b**) Three superimposed sketches of the rat hippocampus from the rostral (back) to caudal (front) regions visually demonstrating the location of PSB-stained recording sites within the CA1 region of the rat hippocampus. (**c**) Two typical photomicrographs, one from the 77-LH-28-1 group and one from the 77-LH-28-1 post-scopolamine group capturing the position of the recording electrodes shown by the location of the PSB stains. 77-LH-28-1, 1-[3-(4-butyl-1-piperidinyl)propyl]-3,4-dihydro-2(1*H*)-quinolinone; PSB, Pontamine Sky Blue.

mAChRs over hM_2–hM_5 receptors, whereas agonists such as carbachol and xanomeline did not. This functional selectivity was also observed in phosphoinositide hydrolysis assays where AC-42 and 77-LH-28-1 increased IP accumulation in CHO-hM_1 cells with pEC_{50} values of 6.1 and 7.4, respectively, but neither stimulated accumulation in CHO-hM_3 cells up to 100 μM. In contrast, carbachol stimulated IP accumulation in both CHO-hM_1 and CHO-hM_3 cells, with similar potencies. It is interesting to note that the potencies of all the agonists tested were reduced in the IP accumulation assay compared with the calcium mobilization readout; this is presumably as a result of the more proximal nature of the IP measurement compared with intracellular calcium mobilization.

The agonist effect of 77-LH-28-1 was blocked by both pirenzepine and scopolamine with affinities in line with their accepted published values at the M_1 mAChR (Ellis, 2002). Analysis of the data sets did not differentiate between a competitive or allosteric mechanism of action of 77-LH-28-1, but validated pirenzepine and scopolamine as tools with

which to inhibit 77-LH-28-1 function in the subsequent native tissue studies.

Compared with the native tissue environment, transfection of recombinant receptors into cells generally results in overexpression, which can generate a large increase in receptor reserve and/or improved receptor-G protein coupling. Therefore, the intrinsic efficacy of an agonist, as measured in recombinant systems, may be overestimated and may not necessarily reflect its activity in a native tissue preparation. To this end, AC-42 and 77-LH-28-1 have been profiled in several rat native tissue systems to understand their functional efficacy at native tissue M_1 mAChRs.

It has been reported that mAChR agonists cause depolarization of hippocampal CA1 pyramidal neurons through activation of M_1 mAChRs (Weiss *et al*., 2000). Indeed, in rat hippocampal slices, carbachol induced pirenzepine-sensitive single-unit firing in the CA1 region, suggesting that it produced its response through activation of M_1 mAChRs. 77-LH-28-1 induced a similar maximal response as carbachol, thus acting as a full M_1 mAChR agonist in this system. However, AC-42 failed to significantly stimulate single-unit cell firing at concentrations up to 30 μM. This suggests that the CA1 cell firing assay is able to functionally discriminate between 77-LH-28-1 and AC-42; the lack of activity of AC-42 is likely to reflect a combination of low potency and efficacy for this compound.

To investigate whether the activity of 77-LH-28-1 resulted from a direct action on the pyramidal cells, or an increase in excitability mediated indirectly through changes in synaptic activity, whole-cell current-clamp recordings from individual CA1 pyramidal neurons were carried out. In these studies, 77-LH-28-1 induced a pirenzepine-sensitive depolarization, suggesting that it produced this response by activation of M_1 mAChRs. Furthermore, 77-LH-28-1 stimulated gamma frequency oscillations in rat hippocampus, a response that is reported to be absent in M_1 mAChR knockout mouse hippocampus (Fisahn *et al*., 2002). These data further support that this synchronous network activity may be important for cellular processes underlying cognitive function and that it is mediated by M_1 mAChRs (Wynn *et al*., 2005).

In summary, we have described the pharmacological profile of AC-42 and 77-LH-28-1 at human recombinant and rat native tissue M_1 mAChRs. In recombinant assay systems, both compounds displayed selective agonist activity at M_1 mAChRs. However, in a hippocampal cell firing assay, only 77-LH-28-1 exhibited robust M_1 mAChR activation, suggesting that this compound represents a better agonist with which to explore M_1 mAChR function in native tissue. Intuitively, one would expect that the high degree of mAChR selectivity of 77-LH-28-1 is derived from an interaction with the M_1 mAChR via an allosteric binding site, as has been described previously for AC-42 (Langmead *et al*., 2006). The interaction of 77-LH-28-1 with the M_2 mAChR has been recently examined, and, in agreement with the studies presented here, 77-LH-28-1 displayed little or no agonist activity at this receptor subtype (May *et al*., 2007). However, it does interact with the M_2 mAChR with low affinity (in agreement with the calcium mobilization data presented in Table 1) and it significantly retards the rate of [^{3}H]*N*-methyl scopolamine dissociation from the M_2 mAChR, indicative of an allosteric mode of action (May *et al*., 2007). Further studies are required to fully define the mechanism of action by which 77-LH-28-1 activates the M_1 mAChR. Should this compound prove to be an allosteric agonist, it is noteworthy that activation of M_1 mAChRs via a non-orthosteric site can drive functional responses in native tissue systems similar to that of orthosteric site agonists.

Furthermore, 77-LH-28-1 acts as a high-efficacy agonist at rat native M_1 mAChRs and can increase network oscillations relevant to cognitive processing that would support the potential use of this mechanism in the treatment of cognitive impairment. Pharmacokinetic and *in vivo* electrophysiological studies demonstrated that 77-LH-28-1 was brain penetrant after subcutaneous administration and activates M_1 mAChRs to stimulate CA1 cell firing *in vivo*. Recent studies have also shown that 77-LH-28-1 can enhance NMDA-mediated neuronal excitation in the rat hippocampus *in vivo* after subcutaneous administration (Mok *et al*., 2007). This effect remained in the presence of the peripherally restricted mAChR antagonist atropine methyl nitrate, suggesting that it is centrally mediated. Taken together, these data highlight the suitability of 77-LH-28-1 as a tool with which to investigate the *in vivo* consequences of selective M_1 mAChR activation.

Acknowledgements

We thank Cindy Bock-Zeigler, Wen Trice, Gina Karavidis and Laura Fisher for the initial screening of 77-LH-28-1.

Conflict of interest

CJL, NEA, CLB, JTB, CHD, ITF, VAHF, JJH, HJH, GAJ, JNCK, AM, RM, NP, JP, CR, KRS, MDW, ZW and JW are all employees of GlaxoSmithKline. RJ is an employee of NeuroSolutions Ltd., a provider of contract electrophysiological assays.

References

Alexander SPH, Mathie A, Peters JA (2007). Guide to receptors and channels (GRAC), 2nd edition (2007 revision). *Br J Pharmacol* **150** (Suppl 1): S1–S168.

Anagnostaras SG, Murphy GG, Hamilton SE, Mitchell SL, Rahnama NP, Nathanson NM *et al.* (2003). Selective cognitive dysfunction in acetylcholine M_1 muscarinic receptor mutant mice. *Nat Neurosci* **6**: 51–58.

Baldwin JM, Schertler GF, Unger VM (1997). An alpha-carbon template for the transmembrane helices in the rhodopsin family of G-protein-coupled receptors. *J Mol Biol* **272**: 144–164.

Bodick NC, Offen WW, Levey AI, Cutler NR, Gauthier SG, Satlin A *et al.* (1997). Effects of xanomeline, a selective muscarinic receptor agonist, on cognitive function and behavioral symptoms in Alzheimer disease. *Arch Neurol* **54**: 465–473.

Bonner TI (1989). The molecular basis for muscarinic receptor diversity. *Trends Neurosci* **12**: 148–150.

Brandish PE, Hill LA, Zheng W, Scolnick EM (2003). Scintillation proximity assay of inositol phosphates in cell extracts: high-throughput measurement of G-protein-coupled receptor activation. *Anal Biochem* **313**: 311–318.

Brown JT, Teriakidis A, Randall AD (2006). A pharmacological investigation of the role of GLUK5 containing receptors in kainate-driven hippocampal gamma band oscillations. *Neuropharmacol* **50**: 47–60.

Caulfield MP, Birdsall NJ (1998). International Union of Pharmacology. XVII. Classification of muscarinic acetylcholine receptors. *Pharmacol Rev* **50**: 279–290.

Cortes R, Probst A, Palacios JM (1987). Quantitative light microscopic autoradiographic localisation of cholinergic muscarinic receptors in the human brain: forebrain. *Neuroscience* **20**: 65–107.

Dean B, Bymaster FP, Scarr E (2003). Muscarinic receptors in schizophrenia. *Curr Mol Med* **3**: 419–426.

Dorje F, Wess J, Lambrecht G, Tacke R, Mutschler E, Brann MR (1990). Antagonist binding profiles of five cloned human muscarinic receptor subtypes. *J Pharmacol Exp Ther* **256**: 727–733.

Ellis J (2002). Muscarinic receptors. In: Pangalos MN, Davies CH (eds). *Understanding G Protein-Coupled Receptors and their Role in the CNS*. Oxford University Press: Oxford, UK. pp 349–371.

Fisahn A, Pike F, Buhi EH, Paulsen O (1998). Cholinergic induction of network oscillations at 40 Hz in the hippocampus *in vitro*. *Nature* **394**: 186–189.

Fisahn A, Yamada M, Duttaroy A, Gan J-W, Deng C-X, McBain CJ *et al*. (2002). Muscarinic induction of hippocampal gamma oscillations requires coupling of the M_1 receptor to two mixed cation currents. *Neuron* **33**: 615–624.

Friedman JI (2004). Cholinergic targets for cognitive enhancement in schizophrenia: focus on cholinesterase inhibitors and muscarinic agonists. *Psychopharmacol* **174**: 45–53.

Gether U (2000). Uncovering molecular mechanisms involved in activation of G protein-coupled receptors. *Endocr Rev* **21**: 90–113.

Hagan JJ, Jansen JHM, Broekkamp CLE (1987). Blockade of spatial learning by the M_1 muscarinic antagonist pirenzepine. *Psychopharmacology (Berlin)* **93**: 470–476.

Hagan JJ, Salamone JD, Simpson J, Iversen SD, Morris RGM (1988). Place navigation in rats is impaired by lesions of the medial septum and diagonal band but not nucleus basalis magnocellularis. *Behav Brain Res* **27**: 9–20.

Hamilton SE, Loose MD, Qi M, Levey AI, Hille B, McKnight GS *et al*. (1997). Disruption of the m1 receptor gene ablates muscarinic receptor-dependent M current regulation and seizure activity in mice. *Proc Natl Acad Sci USA* **94**: 13311–13316.

Harries MH, Samson NA, Cilia J, Hunter AJ (1998). The profile of sabcomeline (SB-202026), a functionally selective M_1 receptor partial agonist, in the marmoset. *Br J Pharmacol* **124**: 409–415.

Heidrich A, Rösler M (1999). Milameline: a nonselective partial muscarinic receptor agonist for the treatment of Alzheimer's disease? *CNS Drug Rev* **5**: 93–104.

Langmead CJ, Fry VA, Forbes IT, Branch CL, Christopoulos A, Wood MD *et al*. (2006). Probing the molecular mechanism of interaction between 4-*n*-butyl-1-[4-(2-methylphenyl)-4-oxo-1-butyl]-piperidine (AC-42) and the muscarinic M_1 receptor: direct pharmacological evidence that AC-42 is an allosteric agonist. *Mol Pharmacol* **69**: 236–246.

Levey AI (2003). Chronically mad as a hatter: anticholinergics and Alzheimer's disease pathology. *Ann Neurol* **54**: 144–146.

Lu Z-L, Saldanha JW, Hulme EC (2001). Transmembrane domains 4 and 7 of the M_1-muscarinic acetylcholine receptor are critical for ligand binding and the receptor activation switch. *J Biol Chem* **276**: 34098–34104.

Maddux JM, Kerfoot EC, Chatterjee S, Holland PC (2007). Dissociation of attention in learning and action: effects of lesions of the amygdale central nucleus, medial prefrontal cortex, and posterior parietal cortex. *Behav Neurosci* **121**: 63–79.

May LT, Avlani VA, Langmead CJ, Herdon HJ, Wood MD, Sexton PM *et al*. (2007). Structure–function studies of allosteric agonism at M_2 muscarinic acetylcholine receptors. *Mol Pharmacol* **72**: 463–476.

Mok NHS, Pardoe J, Fricker A-CC, Davies CH, Watson JM, Kew JNC (2007). Activation of M_1 muscarinic receptors enhances NMDA-receptor function: *in vitro* and *in vivo* findings. *Synapses—From Molecules to Circuits and Behaviour*. Cold Spring Harbour Laboratory: Cold Spring Harbour, USA.

Olianas MC, Maullu C, Adem A, Mulugeta E, Karlsson E, Onali P (2000). Inhibition of acetylcholine muscarinic M_1 receptor function by the M_1-selective ligand muscarinic toxin 7 (MT-7). *Br J Pharmacol* **131**: 447–452.

Paxinos G, Watson C (1986). *The Rat Brain in Stereotaxic Coordinates*. Academic Press: Sydney.

Shapiro MS, Loose MD, Hamilton SE, Nathanson NM, Gomeza J, Wess J *et al*. (1999). Assignment of muscarinic receptor subtypes mediating G-protein modulation of Ca^{2+} channels by using knockout mice. *Proc Natl Acad Sci USA* **96**: 10899–10904.

Shinoe T, Matsui M, Taketo MM, Manabe T (2005). Modulation of synaptic plasticity by physiological activation of M_1 muscarinic acetylcholine receptors in the mouse hippocampus. *J Neurosci* **30**: 11194–11200.

Smith G (1988). Animal models of Alzheimer's disease: experimental cholinergic denervation. *Brain Res* **472**: 103–118.

Spalding TA, Birdsall NJ, Curtis CA, Hulme EC (1994). Acetylcholine mustard labels the binding site aspartate in muscarinic acetylcholine receptors. *J Biol Chem* **269**: 4092–4097.

Spalding TA, Trotter C, Skjaerbaek N, Messier TL, Currier EA, Burstein ES *et al*. (2002). Discovery of an ectopic activation site on the M_1 muscarinic receptor. *Mol Pharmacol* **61**: 1297–1302.

Weiner DM, Meltzer HY, Veinbergs I, Donohue EM, Spalding TA, Smith TT *et al*. (2004). The role of M_1 muscarinic receptor agonism of *N*-desmethylclozapine in the unique clinical effects of clozapine. *Psychopharmacol* **177**: 207–216.

Weiss C, Preston AR, Oh MM, Schwarz RD, Welty D, Disterhof JF (2000). The M_1 muscarinic agonist CI-1017 facilitates trace eyeblink conditioning in aging rabbits and increases the excitability of CA1 pyramidal neurons. *J Neurosci* **20**: 783–790.

Wess J (2003). Novel insights into muscarinic acetylcholine receptor function using gene targeting technology. *Trends Pharmacol Sci* **24**: 414–420.

Wess J (2004). Muscarinic acetylcholine receptor knockout mice: novel phenotypes and clinical implications. *Ann Rev Pharmacol Toxicol* **44**: 423–450.

Wood MD, Murkitt KL, Ho M, Watson J, Brown F, Hunter AJ *et al*. (1999). Functional comparison of muscarinic partial agonists at muscarinic receptor subtypes hM_1, hM_2, hM_3, hM_4 and hM_5 using microphysiometry. *Br J Pharmacol* **126**: 1620–1624.

Wynn JK, Light GA, Breitmeyer B, Nuechterlein KH, Green MF (2005). Event-related gamma activity in schizophrenia patients during a visual backward-masking task. *Am J Psychiatry* **162**: 2330–2336.